Est. 1984

ORIENTAL JOURNAL OF CHEMISTRY

An International Open Access, Peer Reviewed Research Journal

www.orientjchem.org

ISSN: 0970-020 X
CODEN: OJCHEG
2023, Vol. 39, No.(5):
Pg. 1101-1112

Design, Synthesis and Anticancer Properties of Novel Hydrazino-Fused Pyrimidines

SATHISH KUMAR MITTAPALLI[1]*, IFFATH RIZWANA[2], CH. HARI PRASAD MURTHY[3], NIMISHA JAIN[1], SAGAR PAMU[1] and PAWAN KUMAR GUPTA[1]

[1]Department of Pharmaceutical Chemistry, Amity Institute of Pharmacy, Amity University, Gwalior, Madhya Pradesh, India.
[2]Department of Pharmaceutical Chemistry, Deccan School of Pharmacy, Hyderabad, Telangana-500081, India.
[3]Department of Pharmacology, Sri Venkateshwera College of Pharmacy, Hyderabad, Telangana-500081, India.
*Corresponding author E-mail: sattisuma@gmail.com

http://dx.doi.org/10.13005/ojc/390503

(Received: September 04, 2023; Accepted: October 07, 2023)

ABSTRACT

Globally widespread cancer causes an urgent need to develop innovative, more potent drugs that can deliver better therapeutic outcomes. The study aimed to synthesize pyazolo(1,5-a) pyrimidines (5a-5j) and test their cytotoxic properties using DPPH and in vitro anticancer activity using MTT assay. The measured bioactivity scores from -0.5 to 0 and the DPPH assay revealed all except 5c, 5b, and 5h exhibited the lowest inhibition observed when compared with the reference ascorbic acid and cytotoxic assay performed with MCF-7 and HepG-2 cell lines and reported that 5b was a potential candidate towards MCF-7 and 5c showed potent cytotoxicity towards HepG-2. Concluding that the mentioned compounds were reported as potent candidates and good agreement was observed between in vitro and in silico studies.

INTRODUCTION

Protein kinases have emerged as a possible therapeutic targets, with nearly 30 distinct kinase targets being developed for the phase-I trials[1]. The cell cycle regulation and proliferation mainly depend on cyclin-dependent kinases (CDKs). The many biochemical targets are deregulated and there are three approved CDKIs like palbociclib, ribociclib and abemaciclib[2]. Because they are crucial in regulating growth factor signaling, tyrosine kinases are a particularly crucial target and many oncogenic tyrosine kinases catalytic domains ATP binding site is the prime site for the inhibitors[3]. Gefitinib[4], lapatinib[5] is a low molecular weight EGFR/erbB2-tyrosine kinase dual inhibitor that competes with the ATP for blockade of the catalytic domain. Purine is a heterocyclic nucleus present in various antimetabolites and modified at positions 2,4 and 9 in the creation of protein kinase inhibitors. A

quinazoline scaffold with a phenylamino pyrimidine moiety is one of the structural characteristics[6]. Pyrazolo-pyrimidine is a bioisostere of purine[7] was given much consideration while creating anticancer scaffolds, as evidenced by PKI-1668 and erlotinib[9]. Over the past few decades, multifunctional compounds have been employed in treating multi-factorial disorders like cancer. These compounds are generically classed as hybrid and chimerical medications comprising two or more merged pharmacophore groups permitting binding to two or more targets[10]. The rational construction of novel "smart" molecules that keep the pre-selected qualities of the original templates is made possible by combining two or more overlapping pharmacophore groups on the same scaffold. This process also has certain advantages, such as a decreased risk of toxicity and unpleasant responses[11,12].

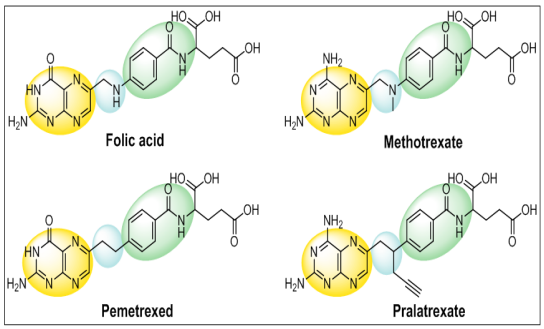

Fig. 1. The features of antimetabolites' structures

Methotrexate, a competitive inhibitor of DHFR that converts DHF to THF, was the foundation for developing the novel pyrazolo(3,4-d) pyrimidines[13]. Recently reported as cytotoxic on BEAS-2B (lung carcinoma) cells, Pemetrexed (PMX) is a dihydropyrrolo[2,3-d]pyrimidin nucleus with ethylene spacer linkage to PABA moiety and acts as a folate antagonist. Studies revealed that the greater affinity complexation of WP6A and ATP favouring competitive replacement of PMX was confirmed by NMR spectroscopy[5]. A folate antagonist previously reported to be an oseltamivir-comparable prospective drug effective against seasonal influenza viruses suppressed SARS-CoV-2 proliferation in Calu-3 cells[14,15].

The epidermal growth factor (EGF) which regulates epithelial cells, the origin of all carcinomas, and the corresponding cell surface receptor are over expressed in tumours and overproduced with mutant hyperactive variants of EGFR being specifically implicated in the promotion of metastasis and tumor growth. A low molecular weight EGFR/erbB2-tyrosine kinase dual inhibitor, gefitinib[4] and lapatinib[5], competes with ATP to block the catalytic domain. Purine is a heterocyclic nucleus found in many antimetabolites and its structural properties include a quinazoline scaffold with a phenylamino pyrimidine moiety and different substituent's at the various positions in the design of protein kinase inhibitors[6]. PKI-166[8], erlotinib[9], imatinib[16], BIRB796[17] and BAY43-9006[18] received significant attention in the development of scaffolds as anticancer medicines.

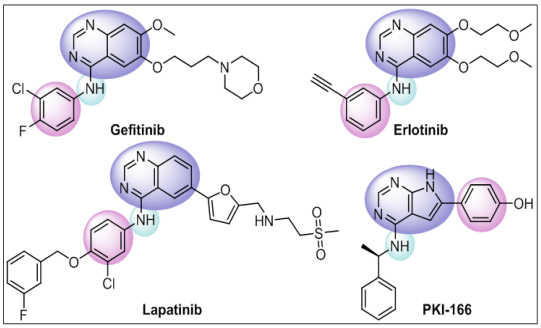

Fig. 2. Inhibitors of the EGFR/erbB2-tyrosine kinase

MATERIALS AND METHODS

Materials

The target proteins were downloaded from the PDB[19] server and Chemdraw Ultra was used to draw the ligand structures. SwissADME[20] utilized to predict the molecular parameters oand molinspiration was one of the web servers to produce the bioactivity scores[21]. Molecular docking simulations were performed by the tool Schrodinger 20.3[22] and the discovery studio visualized by Biovia[23]. All the chemicals availed from Aldrich & SD Fine Chemicals and M.Ps were found using an open capillary tube (Stuart Scientific SMP1). Ethyl acetate and n-butanol (20:80) were used in TLC using precoated silica plates to ensure the purity of the compounds. The infrared spectra in KBr (Vmax in cm^{-1}) were captured using a Shimadzu-FT-IR infrared spectrometer. ^{13}C (100-MHz) & ^{1}H (400-MHz) NMR spectra using Bruker DPX 300 spectrometers using TMS as an internal standard. Thermo Finnigan LCQ Ion Trap & Agilent-1200 series LC instruments were used to collect high-resolution mass spectra, which were then shown in m/z as molecular ion peaks. In order to perform the elemental analysis, VARIO EL-III was employed. Human cell lines from NCCS, Pune, India, include MCF-7 and Hep-G2. Ninety-six

well plates, 25 cm^2 and 75 cm^2 flasks and more from Eppendorf India were purchased.

Evaluation of the molecular descriptive characteristics

In order to anticipate the drug-like properties, which is the key step in the drug development process, the SwissADME online program was used[20]. The main characteristics of a drug candidate are molecular weight, absorption, a limited amount of molecular flexibility and TPSA[24]. It is possible to assess a compound permeability and bioavailability using straight forward molecular information[25]. Based on molecular properties using lipinski's rule of five criteria states that a molecule is a drug like property if it has five hydrogen bond donors, ten hydrogen bond acceptors, five partition coefficients logP, and a molecular weight of 500 daltons[26].

Molecular docking analysis

It has become possible to get the crystal structures of tyrosine kinase and cyclin-dependent kinases from the PDB (ID: 7QHL & 2SRC). The protein structure was constructed using the Schrodinger suite 20.3 tool for protein construction. The protein preparation wizard enabled the energy minimization of the structure the addition of the missed atoms, deletion of water located less than 5 from the binding pocket and the addition of the missing atoms. The grid was created by selecting the co-crystals active location and placing a grid box in its center. The ligands were sketched and energy was minimized, then ligands were made by Lig-Prep Schrodinger module to produce various conformers. The conformers were docked using glide in normal precision mode. The poses were sorted and the top pose was identified. It was known that previous reports stated that co-crystal of target CDK receptor binding modes that the three essential hydrogen binding interactions at active site besides hydrophobic interactions are GLU81, ASP86, and LEU83, and validation was confirmed by redocking of co-crystallized structure with target kinase.

Synthesis protocol

General Procedure for synthesis of pyazolo(3,4-d) pyrimidines

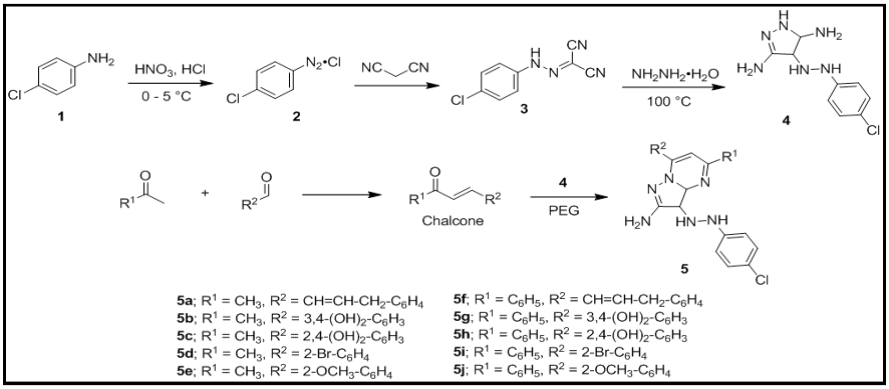

Scheme 1. Representative scheme for the synthesis of Pyrazolopyrimidines

Weigh about 12.77 g (0.1 mol) of 4-Chloro aniline (1), transferred to a beaker and 9.8 mL of nitrous acid was added in cool condition the mixture and kept aside for 30 minutes. By adding 100 mL of ice-cold water to the solid material that had precipitated, it was separated and dried to produce 4-chloro benzene diazonium chloride (2). The compound 2 was taken about 8.5 g (0.05 mol), transferred into R.B.flask and was treated with malononitrile in acetic anhydride under reflux for 5 hrs to afford (4-chlorophenyl)carbonohydrazonoyl dicyanide (3). The compound 3 reacts with hydrazine hydrate in ethyl acetate solution under reflux for 4 h to afford the compound 4-[2-(4-chlorophenyl) hydrazinyl]-4,5-dihydro-1H-pyrazole-3,5-diamine (4). In the next step, chalcones were prepared using different aldehydes and ketones. They obtained chalcones by treating compound 4 independently under magnetic agitation for 6 h in ethanol and drying to afford the compounds 5a-5j.

Biological evaluation

DPPH radical scavenging assay

The imbalance between free radical production and antioxidant defense systems is known as oxidative stress. It is connected to many

pathophysiological conditions, such as cancer and neurological diseases. Antioxidants, whether exogenous or endogenous, enzymatic or non-enzymatic, can reduce or stop cellular damage, primarily through scavenging free radicals. The synthesized compounds were examined for their capacity to scavenge free radicals using the DPPH assay method. In order to create a series of dilutions with concentrations ranging from 100 to 200 µg/mL in methanol. The methanolic solution of the synthesized compound (2 mL) was added to a 0.003% (w/v) methanolic solution of DPPH (1 mL). The mixture was vigorously shaken for five minutes and kept aside for 30 min and measured absobance and ascorbic acid served as the reference at 517nm. The equation used to get the inhibition ratio (%I) for all substances tested is %I=(Ac-As)/Acx100, where Ac is the absorbance of the control and As is the absorbance of the sample[27,28].

MTT Assay for Cytotoxic activity

The MTT assay is a colorimetric technique that measures how much mitochondrial succinate dehydrogenase lowers the yellow dye. The study assumed that a certain number of cells existed and that dead cells in the medium did not diminish the amount of tetrazolium dye and the dye penetrates cells and travel to the mitochondria, where it is transformed into formazan and color intensity measured at 570nm.

The MTT assay was done in triplicates of six independent concn's to predict cell viability and evaluate cell viability in the suspension and trypsinization. The trypan blue test was carried out. The cells were seeded in 96 well plates at a density of $5.0X10^3$ cells per well in 100 mL culture medium and incubated overnight at 37°C. The hemocytometer was used to count the cells. Old media was removed after incubation and replaced with a new medium containing test samples at 5,10,25,50 and 100 µg/mL concentrations. After 48 h, new tetrazolium dye was added and incubated at 37°C for 3 h before the solution's absorbance was measured in a DMSO medium at 570nm[29]. Calculating the growth inhibition percentage involved:

$$\text{Percentage of inhibition} = 100 - \frac{\text{Mean OD of Individual Test Group}}{\text{Mean OD of Control Group}} \times 100$$

Y = mx+C, was used to get the IC_{50} value. Here, the viability graph's Y = 50, M and C values were calculated.

RESULTS AND DISCUSSION

Evaluation of the molecular descriptors

This section lists physical properties and except for a few exempt characteristics like mass and HBA, all the chemicals were within the allowed ranges; all the information was provided in Table 1.

Table 1: Physicochemical properties of the compounds

Title	Chemical	M.Wt	HBD	HBA	LogP	M.R	TPSA[+²]	nrotb	*RO5*
5a	$C_{22}H_{23}ClN_6$	406.91	3	3	3.89	133.24	78.04	6	0
5b	$C_{22}H_{23}ClN_6O_2$	438.92	5	5	3.18	133.72	118.5	6	0
5c	$C_{22}H_{23}ClN_6O_2$	438.92	5	5	3.18	133.72	118.5	6	0
5d	$C_{22}H_{22}BrClN_6$	485.81	3	3	4.81	137.37	78.04	6	1
5e	$C_{23}H_{25}ClN_6O$	436.94	3	4	3.86	136.27	87.28	7	1
5f	$C_{27}H_{25}ClN_6$	468.98	3	3	5.04	149.35	78.25	7	1
5g	$C_{27}H_{25}ClN_6O_2$	500.98	5	5	3.98	153.24	118.52	7	1
5h	$C_{27}H_{25}ClN_6O_2$	500.98	5	5	3.98	153.24	118.52	7	1
5i	$C_{27}H_{24}BrClN_6$	547.88	3	3	5.6	157.05	78.25	7	2
5j	$C_{28}H_{27}ClN_6O$	499.01	3	4	4.7	155.85	87.27	8	1

"M.Wt = Molecular weight; g/mol; HBD=Hydrogen bond donor; HBA=Hydrogen bond acceptor; lipophilicity (expressed as LogP) LogP=implicit logP method; M.R=Molar Refractivity; TPSA=Topological polar surface area; nrotb=no. of rotatable bonds; RO5=no. of Lipinski violation"

Bioactivity Score Calculation Using the Molinespiration Toolkit

Calculate the inhibitory activity against various receptor ligands, inhibitors, and enzymes using the molinspiration online toolbox[21]. Inactivity is expected for scores below -0.50, moderate activity is projected between -0.50 and 0.00 and considerable activity if its bioactivity score is more than 0.00. All data are shown in Table 2.

Table 2. Molinspiration is a measure of the compounds' bioactivity

Title	GPCR ligand	Ion Channel modulator	Kinase inhibitor	Nuclear Receptor ligand	Protease inhibitor	Enzyme inhibitor
5a	-0.09	-0.10	-0.25	-0.52	-0.15	-0.02
5b	-0.14	-0.24	-0.35	-0.68	-0.32	-0.21
5c	-0.24	-0.31	-0.41	-0.69	-0.35	-0.22
5d	-0.27	-0.30	-0.42	-0.87	-0.38	-0.28
5e	-0.3	-0.39	-0.49	-0.85	-0.42	-0.32
5f	-0.1	-0.20	-0.26	-0.54	-0.15	-0.12
5g	-0.11	-0.28	-0.31	-0.64	-0.26	-0.19
5h	-0.19	-0.33	-0.35	-0.65	-0.29	-0.2
5i	-0.22	-0.33	-0.36	-0.79	-0.31	-0.25
5j	-0.25	-0.40	-0.42	-0.78	-0.34	-0.28

Evaluation of the binding energies to biological targets

All the compounds were targeted for biochemical target was chosen as tyrosine-protein kinase SRC (PDB ID:2SRC) with single chain A, length 452, and with the co-crystal structure phosphoraminophosphonic acid-adenylate ester with potential docking score -9.758, and Glide model score -139.143. The target as cyclin-dependent kinase-2 (PDB ID: 7QHL), with chain A & C, length 209, and with co-crystal "5-(2-amino-1-ethyl)thio-3-cyclo-butyl-7-[4-(pyrazolo-1-yl)benzyl]amino-pyrazol[4,3-d]pyrimidine" showed potential docking score -10.765 and Glide modelscore -99.351 and all the data was reported in Table 3.

The compound 5c reported -7.192 (Fig. 3), and 5h reported -7.04K.Cal per mole (Fig. 4) against tyrosine kinase, where the standard doxorubicin and pemetrexed reported -8.814K.Cal per mole showed -7.646 K.Cal per mole respectively (Figure 5 & 6). The reference, doxorubicin scored -8.924 K.Cal per mole against CDKs and pemetrexed which reported -8.34 K.Cal per mole (Fig. 9 & 10), the compounds 5b and 5h exhibited -6.799 (Fig. 7) and -6.915 K.Cal per mole (Figure 8) respectively.

Table 3: Molecular Docking Results targeting 2SRC and 7QHL

Compound Code	2SRC (Tyrosine kinase)		7QHL (Cyclin Dependent Kinase-2)	
	Glide emodel	Docking score	Glide emodel	Docking score
5a	-54.008	-6.099	-55.813	-6.645
5b	-45.255	-4.897	-61.654	-6.799
5c	-66.017	-7.192	-61.081	-6.699
5d	-59.321	-5.973	-54.691	-6.002
5e	-53.516	-5.548	-52.018	-5.915
5f	-62.733	-6.529	-63.604	-6.433
5g	-59.323	-5.641	-62.461	-5.615
5h	-77.117	-7.04	-71.638	-6.915
5i	-63.967	-5.961	-61.406	-5.974
5j	-62.247	-6.3	-67.641	-6.49
Doxorubicin	-95.069	-8.814	-89.171	-8.924
Pemetrexed	-84.831	-7.646	-88.372	-8.34
Co-Crystal	-139.143	-9.758	-99.351	-10.765

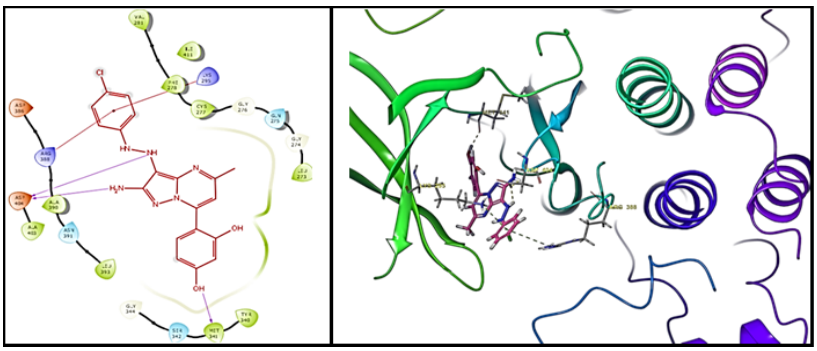

Fig. 3. 2D and 3D mode affections of 5c against 2SRC

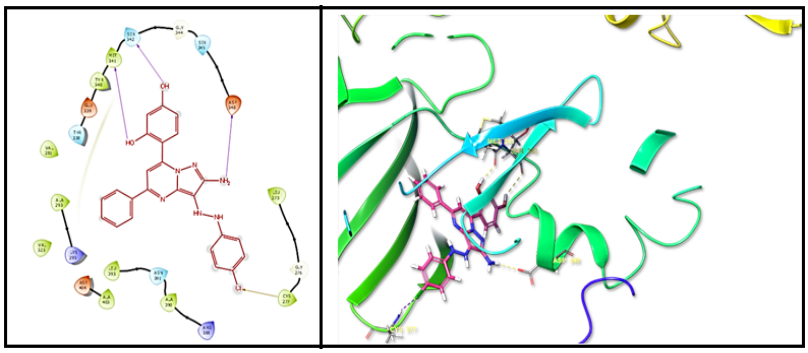

Fig. 4. 2D and 3D mode affections of 5h against 2SRC

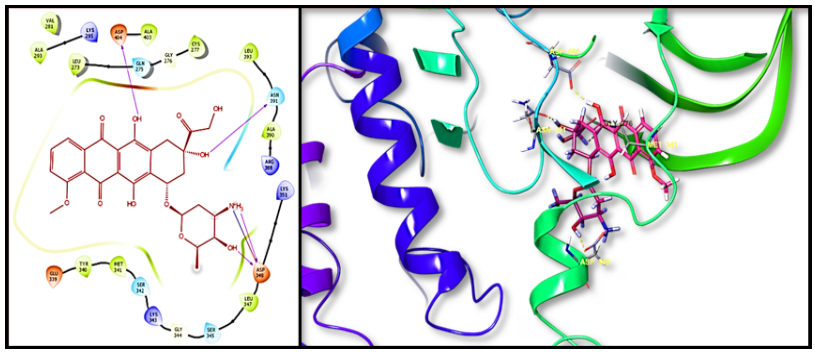

Fig. 5. 2D and 3D mode affections of doxorubicin against 2SRC

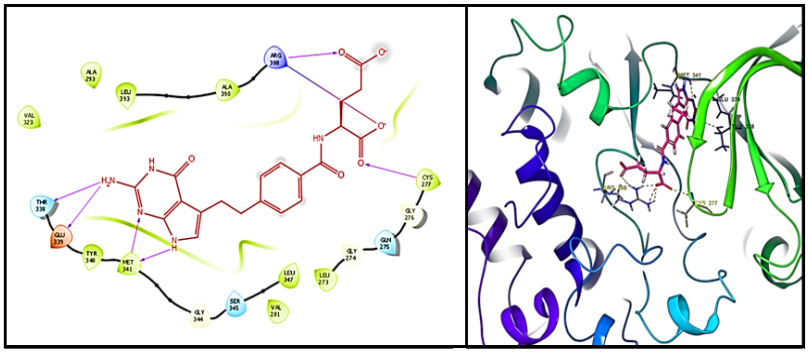

Fig. 6. 2D and 3D mode affections of Pemetrexed against 2SRC

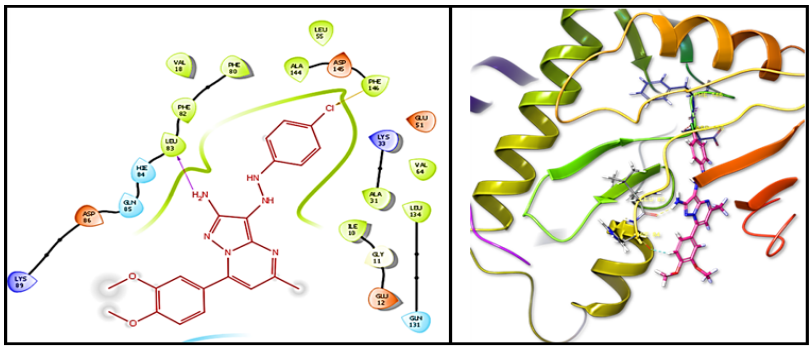

Fig. 7. 2D and 3D mode affections of 5b against 7QHL

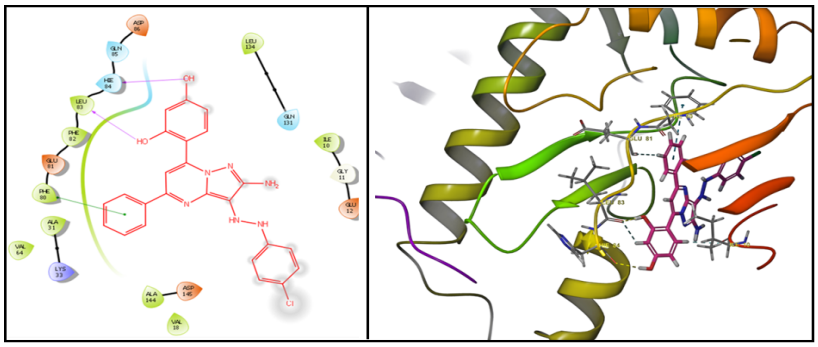

Fig. 8. 2D and 3D mode affections of 5h against 7QHL

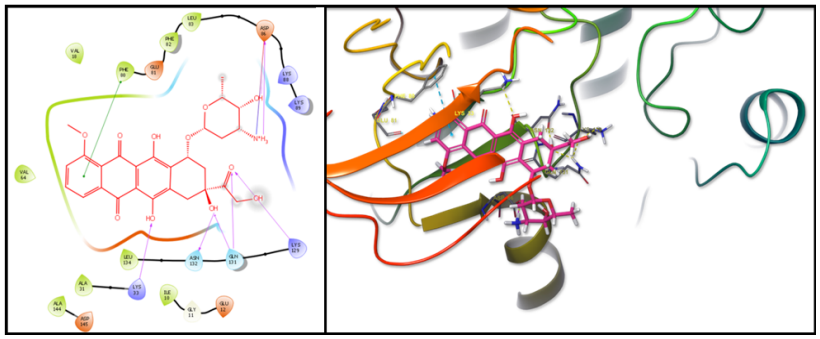

Fig. 9. 2D and 3D mode affections of Pemetrexed against 7QHL

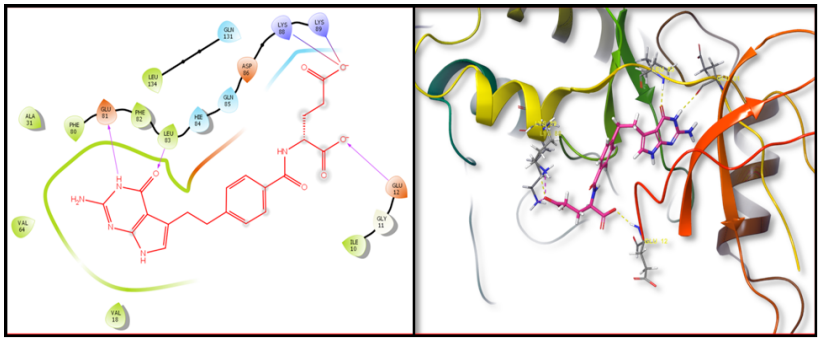

Fig.10. 2D and 3D mode affections of Pemetrexed against 7QHL

Chemistry

Spectral data of the Synthesized Compounds

(4-chlorophenyl)carbonohydrazonoyl dicyanide (3)

Color: White solid; Yield 85%; Melting point: 165-167˚C; FT-IR (cm^{-1}): 3315 (N-H), 3225 (CH–Ar), 1616 (C=N), 1255 (C-N); ^{1}H-NMR: δ 6.69 (m, 2H, *J*=8.4, 1.9, 0.6 Hz), 6.91(s,1H, HC=C), 7.38 (m, 2H, *J*=8.4, 1.7, 0.6 Hz); ^{13}C NMR: δ 15.3, 18.0, 111.3, 114.1, 145.4, 148.1, 148.4; HRMS: *m/z*$[M+H]^+$ Calculated for $C_9H_5ClN_4$ 204.1711, found 204.1725.

4-[2-(4-chlorophenyl)hydrazinyl]-4,5-dihydro-1H-pyrazole-3,5-diamine (4)

Colour: White solid;Yield 88%; Melting point: 220-222˚C; FT-IR (cm^{-1}): 3185 (N-H), 2865 (C-H), 1543 (C=C), 1358 (C-H bending); ^{1}H-NMR: δ 4.15-4.82 (s, 2H, pyrazole), 7.27-7.73 (m, 4H, ArCH, *J*=8.0, 7.5, 1.4 Hz), 12.61 (s, 1H, NH); ^{13}C NMR: δ δ 56.6, 80.5, 117.7, 128.9, 133.7, 148.8, 150.9. HRMS: m/z$[M+H]^+$ Calcd $C_{17}H_{14}N_4O_4$ 240.35,found 240.25.

3-[2-(4-chlorophenyl)hydrazinyl]-5-methyl-7-[2-phenylethenyl]pyrazolo[1,5-a]pyrimidin-2-amine (5a)

Colour: White solid; Yield 71%; Melting point: 268-270˚C; FT-IR (cm^{-1}): 3035 (N-H), 3055 (Ar-CH), 2755(C-H), 1665(C=N), 1525 (Ar-C=C), 726 (C-Cl); ^{1}H-NMR: δ 1.21 (d, 3H, CH_3, *J* = 6.4 Hz),

1.95 (s, 3H, CH_3), 3.51 (d, 1H, *J*=9.2, 6.4 Hz), 4.09 (d, 1H, *J*=7.9 Hz), 4.62 (d, 1H, *J*=7.9 Hz), 5.46 (d, 1H, *J*=9.2 Hz), 6.72 (d, 1H, *J*=17.3 Hz), 6.88 (d, 1H, *J*=17.3 Hz), 7.02-7.25 (m, 3H, *J*=8.2 Hz), 7.26-7.52 (m, 6H, ArH, *J*=7.6, 1.8, 1.3, 0.5 Hz); ^{13}C-NMR: δ 14.5, 22.2, 46.5, 56.6, 80.5, 117.7, 119.5, 123.8, 126.3, 127.2, 127.8, 128.4, 128.9, 130.3, 133.6, 133.8, 148.8, 151.7; HRMS: m/z[M+H]$^+$ Calculated for $C_{22}H_{23}ClN_6$ 406.91, found 406.82; Anal. Calcd C (58.17%), H (6.74%), N (25.47%). Found: C (57.77%), H (6.03%), N (24.84%).

4-[(2-{2-amino-3-[2-(4-chlorophenyl)hydrazinyl]-5-methylpyrazolo[1,5-a]pyrimidin-7-yl}ethenyl] benzene-1,2-diol (5b)

Colour: Brown solid; Yield 68%; Melting point: 275-277˚C; FT-IR (cm^{-1}): 3055 (N-H), 3785 (Ar-CH), 3265 (O-H), 2675 (C-H), 1687 (C=N), 1548 (Ar-C=C), 786 (C-Cl); ^{1}H-NMR: δ 1.21 (d, 3H, CH_3, *J*=6.4 Hz), 1.95 (s, 3H, CH_3), 3.45 (1H, dq, *J*=9.0, 6.4 Hz), 4.09 (1H, d, *J*=7.9 Hz), 4.62 (d, 1H, *J*=7.9 Hz), 5.39 (d, 1H, *J*=9.0 Hz), 6.55-6.72 (m, 2H, CH, *J*=15.5 Hz), 6.86 (d, 1H, *J*=15.5 Hz), 7.02-7.16 (m, 3H, ArH, *J*=8.6, 8.1 Hz), 7.28-7.52 (3H, 7.34 (m, *J*=8.1, 2.5 Hz); ^{13}C NMR: δ 14.5, 22.2, 46.5, 56.6, 80.5, 115.1, 117.7, 119.5, 121.3, 123.8, 126.9, 128.4, 128.9, 129.6, 133.6, 133.8, 133.7, 133.7, 145.6, 146.8, 148.8, 151.7; HRMS: *m/z*[M+H]$^+$ Calculated for $C_{22}H_{23}ClN_6O_2$ 438.92, found 438.54; Clalcd C (68.70%), H (5.77%), N (18.49%). Found: C (67.54%), H (5.19%), N (18.10%).

4-[2-{2-amino-3-[2-(4-chlorophenyl)hydrazinyl]-5-methylpyrazolo[1,5-a]pyrimidin-7-yl}ethenyl] benzene-1,3-diol (5c)

Colour: Light brown solid; Yield 82%; Melting point: above 300˚C; FT-IR (cm^{-1}): 3045 (N-H, str.), 3146 (Ar-CH), 3355 (O-H), 2645 (C-H), 1669 (C=N), 685 (C-Cl); ^{1}H-NMR: δ 2.71 (s,3H, CH_3), 3.78-3.88 (s, 6H, OCH_3, *J*=8.4, 0.5 Hz), 6.97-7.29 (m, 4H, ArCH, *J*=8.4, 1.8 Hz), 7.08-7.96 (m, 3H, ArH, *J*=1.8, 0.5 Hz), 8.62 (s, 1H, CH); ^{13}C-NMR: δ 26.7, 56.0, 56.0, 109.1, 111.2, 115.7, 128.0, 128.1, 128.3, 128.2, 130.1, 131.9, 137.7, 148.2, 148.4, 157.3, 159.0; HRMS: *m/z*[M+H]$^+$ Calculated for $C_{22}H_{23}ClN_6O_2$ 438.92, found 438.54; Anal. Calcd for: C (65.74%), H (6.78%), N (13.51%). Found: C (65.54%), H (5.80%), N (13.05%).

7-[2-(4-bromophenyl)ethenyl]-3-[2-(4-chlorophenyl)hydrazinyl]-5-methylpyrazolo [1,5-a]pyrimidin-2-amine (5d)

Color: Light yellow solid;Yield 62%; Melting point: above 300˚C; FT-IR (cm^{-1}): 2954 (N-H), 3167 (Ar-CH), 2875 (C-H), 1578 (C=N), 824 (C-Cl), 525 (C-Br); ^{1}H-NMR: δ 2.71 (s, 3H, CH_3), 6.97-7.33 (m, 4H, ArH, *J*=8.4, 1.8 Hz), 7.08-7.96 (m, 4H, ArH, *J*=1.8, 0.5 Hz), 8.71 (s, 1H, CH), 9.58 (s, 1H, NH), 11.48 (s, 1H, OH), 13.19 (s, 1H, NH); ^{13}C-NMR: δ 26.7, 115.7, 116.8, 118.9, 128.1-128.3, 128.2, 128.2, 128.2, 128.4, 129.4, 131.9, 132.5, 137.7, 157.3, 161.1, 162.2; HRMS: *m/z* [M+H]$^+$ Calculated for $C_{22}H_{22}BrClN_6$ 485.44, found 485.93; Anal. Calcd: C(66.71%), H(5.48%), N(15.47%). Found: C (66.12%), H (4.10%), N (14.81%).

7-[2-(2-methoxyphenyl)ethenyl]-3-[2-(4-chlorophenyl)hydrazinyl]-5-methylpyrazolo [1,5-a]pyrimidin-2-amine (5e)

Color: Cream color solid;Yield 52%; Melting point: above 300˚C; FT-IR (cm^{-1}): 3045 (N-H), 3052 (Ar-CH), 2755 (C-H), 1654 (C=N), 1011 (C-O), 758 (C-Cl); ^{1}H-NMR: δ 2.75 (s, 3H, CH_3), 6.97-7.33 (m, 4H, ArH, *J*=8.4, 1.8 Hz), 7.08-7.96 (m, 4H, ArH, *J*=1.8, 0.5 Hz), 8.71 (s, 1H, CH), 8.58 (s, 1H, NH), 11.47 (s, 1H, OH), 13.18 (s, 1H, NH); ^{13}C-NMR: δ 26.7, 115.7, 116.8, 118.9, 128.1-128.3, 128.2, 128.2, 128.2, 128.4, 129.4, 131.9, 132.5, 137.7, 157.3, 161.1, 162.2; HRMS: *m/z*[M+H]$^+$ Calculated for $C_{23}H_{25}ClN_6O$ 436.44, found 436.93; Anal. Calcd: C (60.48%), H (4.10%), N (18.71%). Found: C (60.48%), H (4.18%), N (18.08%).

3-[2-(4-chlorophenyl)hydrazinyl]-5-phenyl-7-[(Z)-2-phenylethenyl]pyrazolo[1,5-a]pyrimidin-2-amine (5f)

Color: Brown solid;Yield 75%; Melting point:Melting point: above 300˚C; FT-IR (cm^{-1}): 3155 (N-H), 3175 (Ar-CH), 2784 (C-H), 1555 (C=N), 759 (C-Cl); ^{1}H-NMR: δ 2.73 (s,3H, CH3), 3.78-3.98 (s, 5H, OCH_3, *J*=8.4, 0.4 Hz), 6.97-7.29 (m, 4H, ArCH, *J*=8.4, 1.8 Hz), 7.08-7.97 (m, 3H, ArH, *J*=1.8, 0.5 Hz), 8.65 (s, 1H, CH), 9.58 (s, 1H, NH); ^{13}C-NMR: δ 26.7, 56.0, 56.0, 109.1, 111.2, 115.7, 128.0, 128.1, 128.3, 128.2, 130.1, 131.9, 137.7, 148.2, 148.4, 157.3, 159.0; HRMS: *m/z*[M+H]$^+$ Calculated for $C_{27}H_{25}ClN_6O_2$ 468.98, found 468.41; Anal. Calcd: C (61.47%), H (6.48%), N (12.41%). Found: C (61.14%), H (5.81%), N (13.15%).

4-[(2-{2-amino-3-[2-(4-chlorophenyl) hydrazinyl]-5- phenylpyrazolo[1,5-a]pyrimidin-7-yl}ethenyl]benzene-1,2-diol (5g)

Colour: Yellow solid; Yield 64%; Melting point: above 300˚C; FT-IR (cm^{-1}): 3154 (N-H), 3106

(Ar-CH), 3284(O-H), 2851(C-H), 1671(C=N), 1549 (Ar-C=C), 596 (C-Cl); ^{1}H-NMR: δ 2.81 (s, 3H, CH_3), 6.91-7.33 (m, 4H, ArH, *J*=8.4, 1.8 Hz), 7.08-7.96 (m, 4H, ArH, *J*=1.8, 0.5 Hz), 8.71 (s, 1H, CH), 9.58 (s, 1H, NH), 13.18 (s, 1H, NH), 13.19 (s, 1H, NH); ^{13}C-NMR: δ 26.7, 115.7, 116.8, 118.9, 128.1-128.3, 128.2, 128.2, 128.2, 128.4, 129.4, 131.9, 132.5, 137.7, 157.3, 161.1, 162.2; HRMS: *m/z* $[M+H]^+$ Calculated for $C_{27}H_{25}ClN_6O_2$ 500.38, found 500.18; Anal. Calcd: C (54.23%), H (4.25%), N (12.65%). Found: C (54.08%), H (4.19%), N (12.08%).

4-[2-{2-amino-3-[2-(4-chlorophenyl)hydrazinyl]-5-phenylpyrazolo[1,5-a]pyrimidin-7-yl}ethenyl] benzene-1,3-diol (5h)

Colour: Light yellow solid; Yield 71%; Melting point: above 300˚C; FT-IR (cm^{-1}): 3148 (N-H), 3087 (Ar-CH), 3255 (OH), 2761(C-H), 1685 (C=N), 856 (C-Cl); ^{1}H-NMR: δ 3.78-3.88 (s, 6H, OCH_3), 6.98-7.97 (m, 10H, ArH, *J*=8.4, 1.8 Hz), 8.6 (s, 1H, CH), 8.63 (s, 1H, CH), 9.58 (s, 1H, NH); ^{13}C-NMR: δ 56.0, 111.2, 115.7, 119.9, 127.8, 128.0, 128.1, 128.3, 128.2, 130.1, 131.9, 134.2, 137.7, 148.2, 148.4, 153.0, 159.0; HRMS: *m/z* $[M+H]^+$ Calculated for $C_{27}H_{25}ClN_6O_2$ 500.88, found 500.98; Anal. Calcd: C (70.38%), H (5.64%), N (11.19%). Found: C (70.10%), H (5.18%), N (11.84%).

7-[2-(4-bromophenyl)ethenyl]-3-[2-(4-chlorophenyl)hydrazinyl]-5-phenylpyrazolo [1,5-a]pyrimidin-2-amine (5i)

Colour: White solid; Yield 59%; Melting point: above 300˚C; FT-IR (cm^{-1}): 2967 (N-H), 3185 (Ar-CH), 2853(C-H), 1665 (C=N), 1529 (Ar-C=C), 794 (C-Cl), 585 (C-Br); ^{1}H-NMR: δ 2.71 (s, 3H, CH_3), 6.90-7.39 (m, 4H, ArH, *J*=8.4, 1.8 Hz), 7.08-7.96 (m, 4H, ArH, *J*=1.8, 0.5 Hz), 8.71 (s, 1H, CH), 9.58 (s, 1H, NH), 11.45 (s, 1H, OH), 13.18 (s, 1H, NH), 13.19 (s, 1H, NH); ^{13}C-NMR: δ 26.7, 115.7, 116.8, 118.9, 128.1, 128.3, 128.2, 128.2, 128.4, 129.4, 131.9, 132.5, 137.7, 157.3, 161.1, 162.2; HRMS: *m/z* $[M+H]^+$ Calculated for $C_{27}H_{24}BrClN_6$ 547.88, found 547.14; Anal. Calcd: C (72.49%), (5.17%), N (12.68%). Found: C (72.19%), H (5.10%), N (12.27%).

7-[2-(2-methoxyphenyl)ethenyl]-3-[2-(4-chlorophenyl)hydrazinyl]-5-phenyl pyrazolo [1,5-a]pyrimidin-2-amine (5j)

Color: Pinkish brown solid; Yield 62%; Melting point: above 300˚C; FT-IR (cm^{-1}): 3017 (N-H), 3084 (Ar-CH), 2784(C-H), 1664 (C=N), 1548 (Ar-C=C), 1087 (C-O-C), 657 (C-Cl); ^{1}H-NMR: δ 2.71 (s, 3H, CH_3), 6.90-7.39 (m, 4H, ArH, *J*=8.4, 1.8 Hz), 7.08-7.96 (m, 4H, ArH, *J*=1.8, 0.5 Hz), 8.71 (s, 1H, CH), 9.42 (s, 1H, NH), 11.45 (s, 1H, OH), 13.18 (s, 1H, NH), 13.19 (s, 1H, NH); ^{13}C-NMR: δ 26.7, 115.7, 116.8, 118.9, 128.1, 128.3, 128.2, 128.2, 128.4, 129.4, 131.9, 132.5, 137.7, 157.3, 161.1, 162.2; HRMS: *m/z* $[M+H]^+$ Calculated for $C_{28}H_{27}ClN_6O$ 499.09, found 499.01; Anal. Calcd: C (72.41%), (5.08%), N (12.52%). Found: C (72.03%), H (5.92%), N (12.08%).

4-Chloro aniline (1), upon diazotization reaction in the presence of nitrous acid at 0-5°C to give compound 2 and followed by treatment with malononitrile in acetic anhydride to afford (4-chlorophenyl)carbonohydrazonoyl dicyanide (3), which upon treated with hydrazine hydrate to afford the compound 4-[2-(4-chlorophenyl)hydrazinyl]-4,5-dihydro-1H-pyrazole-3,5-diamine (4), which was condensed with chalcones to afford the compounds 5a-5j, as shown in the Scheme 1. The compounds 5a-5j were obtained in moderate to good yields (52-82%) and recrystallized from ethanol and ethyl acetate. The analogues IR spectra showed the existence of C=N bonds in the 1525–1685 cm^{-1} area, two NH bonds in the 2900–3150 cm^{-1} region, OH groups in the 3200–3500 cm^{-1} region, C–Cl bonds in the 560-850 cm^{-1} region, and C–Br bonds in the 525–585 cm^{-1} region. In ^{1}H-NMR spectra, a singl *et at.*, δ 1.75 to 2.85 ppm assignable for a methyl group, singlet at δ 3.78-3.88 for methoxy protons, singlet for NH protons δ 7.78-8.55 for hydrazine protons and multiplet for protons in aromatic region at δ 7.08-8.5 in ^{13}C-NMR spectra aromatic carbons revealed at a range of 120-155 ppm, and the pyrazolopyrimidine scaffold carbons absorb at 90-160 ppm region. Moreover, the HRMS and elemental analysis were carried out to confirm the novel compounds.

Biological Evaluation

The scavenging effect percentage of the compound 5 h at 100, 150, and 200 µg/mL is 51.4, 60.2, and 68.3. The scavenging property of 5b at 100, 150, and 200 µg/mL is 51.5, 62 and 67.8 respectively. Ascorbic acid demonstrated a 98.3% scavenging efficiency at a 200 µg/mL concentration. The good inhibition of 5c showed 52.8, 62.5, and 69.4% at 100, 150 and 200 µg/mL respectively. All the compounds except 5c, 5b, and 5h exhibited lowest inhibition. The electron-donating hydroxyl groups in the compounds 5c, 5b, and 5h exhibited the highest antioxidant activities compared to other compounds. Table 4 displays the RSC as a percentage.

Table 4: Radical Scavenging Activity in DPPH

Compound	The concentration of the tested compounds (µg/ml) 100	150	200
5a	12.8	18.3	27.6
5b	51.5	62	67.8
5c	52.8	62.5	69.4
5d	20.7	34.8	38.7
5e	54.8	46.4	54.7
5f	32.5	46.8	52.6
5g	22.5	32.4	39.4
5h	51.4	60.2	68.3
5i	21.7	37.7	39.1
5j	37.3	47.5	53.9
Ascorbic acid	73.3	85.6	98.3

Using the MTT assay, the cytotoxic effects of each substance were examined against the MCF-7 and HepG-2 cell lines. The cytotoxicity was assessed using various concentrations and 5-FU as the standard drug. The consolidated concentrations of compounds with respect to inhibition percentage as well as cell viability against MCF-7 and Hep G2were given in Table 2. For *in vitro* anticancer investigations, every chemical underwent screening. The cytotoxic evaluations were done MTT assay revealed that the compounds 5b (Graph-1 & Table 7) reported as potential against MCF 7 with the IC_{50}, 16.61 followed by 5d with the IC_{50} 19.67 µg/mL, where the standard reference showed 14.34 µg/m and 5c (Graph-2 & Table 8) reported as potential against Hep G2 with the IC_{50}, 14.32 µg/mL. This was followed by 5h with the IC_{50} 19.24 µg/mL, where the standard reported 11.36 µg/mL, and all cell viability studies were reported in Table 5.

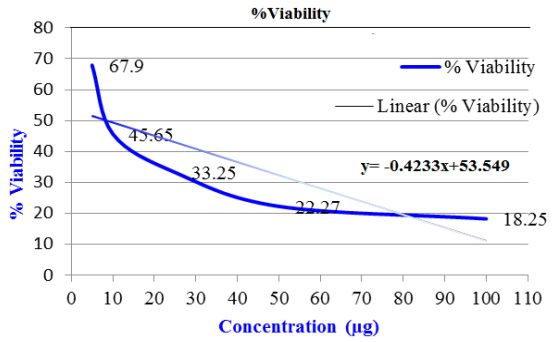

Graph 1: % Viability of 5b against MCF-7

Table 5: *In-vitro* anticancer MTT assay

S. No	Compound	IC_{50} (µg) MCF 7	Hep G2
1	5a	59.65	45.85
2	5b	16.61	22.36
3	5c	>100	14.32
4	5d	19.67	56.82
5	5e	>100	>100
6	5f	29.31	49.25
7	5g	>100	55.37
8	5h	35.35	19.24
9	5i	39.08	>100
10	5j	24.36	34.65
11	5-FU	14.34	11.36

Table 6: Cytotoxicity of 5b against MCF-7 at independent concentrations

Concn (µg)	Abs at 570nm	%Inhbn	%Viability	IC_{50}(µg)
5	0.435	32.1	67.9	16.61
10	0.351	54.35	45.65	
25	0.221	62.73	33.25	
50	0.235	77.73	22.27	
100	0.338	71.36	18.25	
Untreated	0.628	0	100	
Blank	0	0	0	

Table 7: Cytotoxicity of 5-FU against MCF-7

Concn (µg)	Abs at 570nm	%Inhbn	%Viability	IC_{50}(µg)
5	0.586	78.09	21.91	14.32
10	0.435	82.24	17.76	
25	0.362	64.24	35.76	
50	0.321	41.07	58.93	
100	0.376	27.27	72.73	
Untreated	0.743	0	100	
Blank	0	0	0	

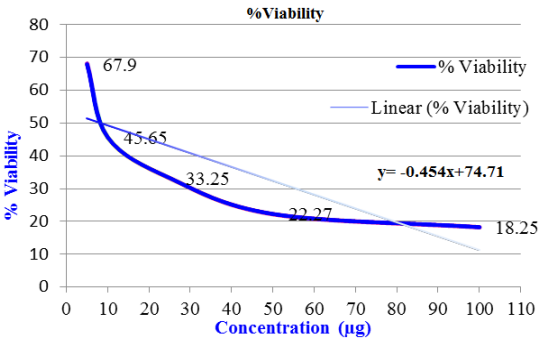

Graph 2: % Viability of 5c against HepG-2

CONCLUSION

As a result, many new pyrazolo(1,5-a) pyrimidines (5a–5j) were synthesized with excellent yield and identified using various spectral methods. All the compounds were evaluated for antioxidant studies, which revealed that compounds 5c, 5b and 5h were potential candidates due to the electron-donating hydroxyl groups being crucial for potency. Also evaluated for cytotoxic MTT assay revealed that the compounds 5b and 5d were potent against MCF-7, and 5c and 5h were potential candidates against HepG-2 cell lines. Some compounds showed mild to moderate cell viability compared with reference

compounds, and compounds 5c and 5h had potential against tyrosine kinase and CDKs.

ACKNOWLEDGMENTS

The Amity University management in Madhya Pradesh has allowed the writers to conduct this study for which the authors are grateful.

Conflict of Interest

There are no competing interests to declare, according to the authors.

REFERENCES

1. Venkanna A.; Subedi L.; Teli MK.; Lama PD.; Nangunuri BG.; Lee SY.; Kim SY.; Kim MH. Positioning of an unprecedented spiro [5.5] undeca ring system into kinase inhibitor space. *Scientific Reports*., **2020**, *10*(1), 21265.
2. Zhang M.; Zhang L.; Hei R.; Li X.; Cai H.; Wu X.; Zheng Q.; Cai C. CDK inhibitors in cancer therapy, an overview of recent development. *American journal of cancer research*., **2021**, *11*(5), 1913.
3. Beretta GL.; Cassinelli G.; Pennati M.; Zuco V.; Gatti L. Overcoming ABC transporter-mediated multidrug resistance: The dual role of tyrosine kinase inhibitors as multitargeting agents. *European journal of medicinal chemistry*., **2017**, *142*, 271-89.
4. Dhillon S. Gefitinib: a review of its use in adults with advanced non-small cell lung cancer. *Targeted oncology*. **2015**, *10*, 153-70.
5. Li X.; Yang C.; Wan H.; Zhang G.; Feng J.; Zhang L.; Chen X.; Zhong D.; Lou L.; Tao W.; Zhang L. Discovery and development of pyrotinib: A novel irreversible EGFR/HER2 dual tyrosine kinase inhibitor with favorable safety profiles for the treatment of breast cancer. *European Journal of Pharmaceutical Sciences*., **2017**, *110*, 51-61.
6. Park H.; Lee H.; Seok C. High-resolution protein–protein docking by global optimization: recent advances and future challenges. *Current opinion in structural biology*., **2015**, *35*, 24-31.
7. Kovalova M.; Havlícek L.; Djukic S.; Skerlova J.; Perina M.; Pospísil T.; Reznícková E. Characterization of new highly selective pyrazolo [4, 3-d] pyrimidine inhibitor of CDK7. *Biomedicine & Pharmacotherapy*., **2023**, *161*, 114492.
8. Matada GS.; Dhiwar PS.; Abbas N.; Singh E.; Ghara A.; Patil R.; Raghavendra NM. Pharmacophore modeling, virtual screening, molecular docking and dynamics studies for the discovery of HER2-tyrosine kinase inhibitors: An in-silico approach. *Journal of Molecular Structure*., **2022**, *1257*, 132531.
9. Barr Kumarakulasinghe N.; Zanwijk NV.; Soo RA. Molecular targeted therapy in the treatment of advanced stage non‐small cell lung cancer (NSCLC). *Respirology*., **2015**, *20*(3), 370-8.
10. Talevi A. Multi-target pharmacology: possibilities and limitations of the "skeleton key approach" from a medicinal chemist perspective. *Frontiers in pharmacology*., **2015**, *6*, 205.
11. Smith EL.; Harrington K.; Staehr M.; Masakayan R.; Jones J.; Long TJ.; Ng KY.; Ghoddusi M.; Purdon TJ.; Wang X.; Do T. GPRC5D is a target for the immunotherapy of multiple myeloma with rationally designed CAR T cells. *Science translational medicine*., **2019**, *11*(485), 7746.
12. Kontoyianni M. Docking and virtual screening in drug discovery. Proteomics for drug discovery: *Methods and protocols*., **2017**, 255-66.
13. Rafique B.; Khalid AM.; Akhtar K.; Jabbar A. Interaction of anticancer drug methotrexate with DNA analyzed by electrochemical and spectroscopic methods. *Biosensors and Bioelectronics*., **2013**, *44*, 21-6.
14. Chen Y.; Zhou X. Research progress of mTOR inhibitors. *European journal of medicinal chemistry*., **2020**, *208*, 112820.
15. Bae JY.; Lee GE.; Park H.; Cho J.; Kim J.; Lee J.; Kim K.; Kim JI.; Park MS. Antiviral efficacy of Pralatrexate against SARS-CoV-2. *Biomolecules & Therapeutics*., **2021**, *29*(3), 268.
16. Estey E.; Levine RL.; Lowenberg B. Current challenges in clinical development of "targeted therapies": the case of acute myeloid leukemia. Blood, *The Journal of the American Society of Hematology*., **2015**, *125*(16), 2461-6.
17. Jin X.; Mo Q.; Zhang Y.; Gao Y.; Wu Y.; Li J.; Hao X.; Ma D.; Gao Q.; Chen P. The p38 MAPK inhibitor BIRB796 enhances the antitumor effects of VX680 in cervical cancer. *Cancer biology & therapy*., **2016** May *3;17*(5), 566-76.
18. Murphy EJ.; Booth JC.; Davrazou F.; Port AM.; Jones DN. Interactions of Anopheles gambiae odorant-binding proteins with a human-derived repellent: implications for the mode of action of n, n-diethyl-3-methylbenzamide (DEET). *Journal of Biological Chemistry*. **2013**, *288*(6), 4475-85.

19. Burley SK.; Bhikadiya C.; Bi C.; Bittrich S.; Chen L.; Crichlow GV.; Duarte JM.; Dutta S.; Fayazi M.; Feng Z.; Flatt JW. RCSB Protein Data Bank: Celebrating 50 years of the PDB with new tools for understanding and visualizing biological macromolecules in 3D. *Protein Science*., **2022**, *31*(1), 187-208.
20. Daina A.; Michielin O.; Zoete V. SwissADME: a free web tool to evaluate pharmacokinetics, drug-likeness and medicinal chemistry friendliness of small molecules. *Scientific reports*., **2017**, *7*(1), 42717.
21. Cheminformatics M. Molinspiration. Molinspiration Cheminformatics., **2010**.
22. Forli S.; Huey R.; Pique ME.; Sanner MF.; Goodsell DS.; Olson AJ. Computational protein–ligand docking and virtual drug screening with the AutoDock suite. *Nature protocols*., **2016**, *11*(5), 905-19.
23. BIOVIA DS. Discovery studio modeling environment, release 2017, San Diego: DassaultSystèmes, 2016. Available from:(Accessed 1 September 2016). **2016**.
24. Sharma T.; Jana S. Investigation of molecular properties that influence the permeability and oral bioavailability of major δboswellic acids. *European Journal of Drug Metabolism and Pharmacokinetics*., **2020**, *45*, 243-55.
25. Castillo-Garit JA.; Casanola-Martin GM.; Le-Thi-Thu H.; Barigye SJ. A simple method to predict blood-brain barrier permeability of drug-like compounds using classification trees. *Medicinal Chemistry*., **2017**, *13*(7), 664-9.
26. Attique SA.; Hassan M.; Usman M.; Atif RM.; Mahboob S.; Al-Ghanim KA.; Bilal M.; Nawaz MZ. A molecular docking approach to evaluate the pharmacological properties of natural and synthetic treatment candidates for use against hypertension. *International journal of environmental research and public health*., **2019**, *16*(6), 923.
27. Ganapathy M, Bhunia S. Nutraceuticals: The new generation therapeutics. *Adv Tech Biol Med*., **2016**, *4*(179), 2379-1764.
28. Kehrer JP, Klotz LO. Free radicals and related reactive species as mediators of tissue injury and disease: implications for health. *Critical reviews in toxicology*., **2015**, *45*(9), 765-98.
29. Huang S, Wang DI, Zhang S, Huang X, Wang D, Ijaz M, Shi Y. Tunicamycin potentiates paclitaxel-induced apoptosis through inhibition of PI3K/AKT and MAPK pathways in breast cancer. *Cancer Chemotherapy and Pharmacology*., **2017**, *80*, 685-96.